



HAL
open science

The role of quantitative markers in surgical prognostication after stereoelectroencephalography

Julia Makhalova, Tanguy Madec, Samuel Medina Villalon, Aude Jegou, Stanislas Lagarde, Romain Carron, Didier Scavarda, Elodie Garnier, Christian G Bénar, Fabrice Bartolomei

► To cite this version:

Julia Makhalova, Tanguy Madec, Samuel Medina Villalon, Aude Jegou, Stanislas Lagarde, et al.. The role of quantitative markers in surgical prognostication after stereoelectroencephalography. *Annals of Clinical and Translational Neurology*, 2023, 10 (11), pp.2114-2126. 10.1002/acn3.51900 . hal-04556224

HAL Id: hal-04556224

<https://amu.hal.science/hal-04556224>

Submitted on 23 Apr 2024

HAL is a multi-disciplinary open access archive for the deposit and dissemination of scientific research documents, whether they are published or not. The documents may come from teaching and research institutions in France or abroad, or from public or private research centers.

L'archive ouverte pluridisciplinaire **HAL**, est destinée au dépôt et à la diffusion de documents scientifiques de niveau recherche, publiés ou non, émanant des établissements d'enseignement et de recherche français ou étrangers, des laboratoires publics ou privés.

RESEARCH ARTICLE

The role of quantitative markers in surgical prognostication after stereoelectroencephalography

Julia Makhlova^{1,2,3} , Tanguy Madec¹, Samuel Medina Villalon^{1,2}, Aude Jegou², Stanislas Lagarde^{1,2} , Romain Carron⁴, Didier Scavarda⁵, Elodie Garnier², Christian G. Bénar² & Fabrice Bartolomei^{1,2} 

¹APHM, Timone Hospital, Epileptology and Cerebral Rhythmology, Marseille, France

²Aix Marseille Univ, INSERM, INS, Inst Neurosci Syst, Marseille, France

³Aix Marseille Univ, CNRS, CRMBM, Marseille, France

⁴APHM, Timone Hospital, Functional, and Stereotactic Neurosurgery, Marseille, France

⁵APHM, Department of Pediatric Neurosurgery, Marseille, France

Correspondence

Fabrice Bartolomei, Service d'Epileptologie et de Rythmologie cérébrale, Hôpital Timone, 264 Rue Saint-Pierre, 13005, Marseille, France. Tel: +33491385833; Fax: +33491385826; E-mail: fabrice.bartolomei@ap-hm.fr

Received: 18 July 2023; Revised: 26 August 2023; Accepted: 8 September 2023

Annals of Clinical and Translational Neurology 2023; 10(11): 2114–2126

doi: 10.1002/acn3.51900

Abstract

Objective: Stereoelectroencephalography (SEEG) is the reference method in the presurgical exploration of drug-resistant focal epilepsy. However, prognosticating surgery on an individual level is difficult. A quantified estimation of the most epileptogenic regions by searching for relevant biomarkers can be proposed for this purpose. We investigated the performances of ictal (Epileptogenicity Index, EI; Connectivity EI, cEI), interictal (spikes, high-frequency oscillations, HFO [80–300 Hz]; Spikes × HFO), and combined (Spikes × EI; Spikes × cEI) biomarkers in predicting surgical outcome and searched for prognostic factors based on SEEG-signal quantification. **Methods:** Fifty-three patients operated on following SEEG were included. We compared, using precision-recall, the epileptogenic zone quantified using different biomarkers (EZ_q) against the visual analysis (EZ_C). Correlations between the EZ resection rates or the EZ extent and surgical prognosis were analyzed. **Results:** EI and Spikes × EI showed the best precision against EZ_C (0.74; 0.70), followed by Spikes × cEI and cEI, whereas interictal markers showed lower precision. The EZ resection rates were greater in seizure-free than in non-seizure-free patients for the EZ defined by ictal biomarkers and were correlated with the outcome for EI and Spikes × EI. No such correlation was found for interictal markers. The extent of the quantified EZ did not correlate with the prognosis. **Interpretation:** Ictal or combined ictal–interictal markers overperformed the interictal markers both for detecting the EZ and predicting seizure freedom. Combining ictal and interictal epileptogenicity markers improves detection accuracy. Resection rates of the quantified EZ using ictal markers were the only statistically significant determinants for surgical prognosis.

Introduction

Epilepsy surgery is the only potential curative treatment for patients suffering from drug-resistant focal epilepsy. Stereoelectroencephalography (SEEG) has become the reference method in invasive presurgical exploration.¹ However, the percentage of patients cured by surgery following SEEG exploration remains limited to 50–60% of cases.^{2,3} There is robust evidence that seizure generation and

propagation occur within patient-specific epileptogenic networks through synchronizing activity between the brain areas (nodes of the network) characterized by altered excitability and connectivity.^{4–6} Epilepsy surgery aims at localizing the brain regions capable of generating seizures (further referred to as the epileptogenic zone network, EZN⁵) and the resection or disconnection of these nodes.⁷

Surgical prognosis may be linked to general disease-related factors such as age, duration of epilepsy,

etiology,⁸ and more specific factors, namely the extent of the EZ resection, which might be impacted by functional constraints.¹ However, individual prognostication of seizure outcome remains difficult due to the great variability of data and the multitude of unknown parameters in many cases.^{7,9} The EZN quantification could facilitate SEEG interpretation and help to establish surgical decision based on objective criteria.^{10–12} Seizures, interictal spikes, and high-frequency oscillations (HFOs, 80–500 Hz) are recognized as electrophysiological biomarkers of the EZN.^{13,14} Ictal epileptogenicity measures quantify the spectral content of SEEG signals and/or changes in functional connectivity at seizure onset. The Epileptogenicity Index (EI)¹⁵ is the first and so far the most routinely used SEEG signal quantification approach. The EI estimates epileptogenicity of brain regions based on their capacity to generate fast discharges at seizure onset and the dynamics of involvement of each respective region during the seizure. Following the EI, other ictal signal quantification methods have emerged, based on the detection of fast activities, eventually in combination with other metrics, such as statistical parametric mapping of gamma power in the epileptogenicity maps method,¹⁶ preictal spiking, and suppression of low frequencies in the fingerprint¹⁷ or slow polarizing shift in the method proposed by Gnatkovsky et al.^{18,19} However, a large part of these methods are less suited for seizure-onset patterns without low-voltage fast activity. The Connectivity Epileptogenicity Index (cEI)²⁰ has been recently developed to overcome this limitation. It combines the original EI quantification with functional connectivity analysis²¹ at seizure onset. In parallel, quantification of interictal epileptogenicity markers, such as spikes, HFOs, or a combination of both, have been tested in several studies, with controversial results regarding their capacity to accurately delineate the epileptogenic from the propagation regions. HFOs were shown to predict surgery outcomes at group level but these findings could not be reproduced on an individual level.^{22–24} Furthermore, spikes and fast ripples (FR, 250–500 Hz) have been suggested as more specific biomarkers of the EZN²⁵ than ripples (80–250 Hz) that may also represent physiological brain activity.²⁶ However, the FR quantification requires a high sampling rate, not always routinely available.

While previous studies have implemented either ictal^{17,20,27–29} or interictal biomarkers,^{23,24,30–33} a systematic comparison of the quantified ictal data using different epileptogenicity markers with interictal markers and clinical analysis has not been performed. Moreover, the plus-value of combining interictal and ictal biomarkers in a single measure as well as the predictive value of different biomarkers for surgical prognosis remain unknown.

In the present study, we sought to assess the performances of ictal (EI, cEI), interictal (spikes, HFO, spikes × HFO), and combined (spikes × EI, spikes × cEI) SEEG biomarkers in predicting surgical outcome and establish factors predictive of surgical prognosis based on SEEG-signal quantification.

Methods

Patient and data collection

Patients were included retrospectively from the database of the Epileptology department, Timone Hospital, Marseille, according to the following criteria: all consecutive patients with drug-resistant focal epilepsy who underwent SEEG exploration followed by curative surgery between June 2012 and June 2019, with available postoperative brain MRI and a postsurgical follow-up of at least 1 year. Presurgical work-up included detailed medical history, neurological examination, neuropsychological testing, FDG-PET, high-resolution 3T MRI, long-term scalp-video-EEG, and SEEG recordings in all patients. A postoperative 3T MRI was performed three months after surgery. The T1-weighted magnetization-prepared rapid gradient echo (T1 MPRAGE) sequences (spatial resolution = $(1.0 \times 1.0 \times 1.0)$ mm³) from pre-SEEG and postoperative MRI were used for the study. Clinical data and follow-up information were collected from the medical records. Surgical outcome was assessed according to Engel classification at last clinical follow-up. All patients have given informed written consent and the study was approved by the Assistance Publique – Hôpitaux de Marseille (health data access portal registration number PADS23-41).

SEEG recording

SEEG recordings were performed as a part of routine presurgical assessment according to the French guidelines.³⁴ Implantation was planned individually for each patient based on the hypotheses about the localization of the EZ formulated from noninvasive data. All SEEG explorations were bilateral, predominant on the side of the main EZ hypothesis, with contralateral sentinel electrodes. Intracerebral multiple contact electrodes (10–18 contacts with length 2 mm, diameter 0.8 mm, and 1.5 mm apart, Alcis or Dixi, France) were placed stereotactically.³⁵ A postimplantation CT was performed to exclude intracranial bleeding and reconstruct the positions of the electrodes. Signals were recorded on a Natus system with sampling at 512 or 1024 Hz and 16-bit resolution using a hardware high-pass filter (cutoff at 0.16 Hz at –3 dB) and a hardware anti-aliasing low-pass filter (cutoff at 200 or 340 Hz, respectively).

SEEG-signal analysis

All signal analyses were computed using the open-source AnyWave software³⁶ available at <https://meg.univ-amu.fr/wiki/AnyWave>. For each patient, a bipolar montage including all contacts within the gray matter was automatically generated using GARDEL software³⁷ available at <https://meg.univ-amu.fr/wiki/GARDEL:presentation>. Channels containing artifacts were excluded by visual inspection.

Ictal epileptogenicity markers (Fig. 1A) included EI¹⁵ and cEI²⁰ and were quantified on two spontaneous seizures per patient. If two or more seizure types were present, at least one representative seizure of each type was analyzed. A dedicated Matlab plug-in was used (cEI plug-

in, <https://meg.univ-amu.fr/wiki/AnyWave:Plug-ins>) to calculate both markers simultaneously. A 30-second analysis window was used, starting 3 seconds before the electrical seizure onset defined by visual analysis (onset of low-voltage fast discharge when present, or onset of rhythmic sustained discharge for seizure-onset patterns of lower frequency). The EI was computed as described elsewhere.¹⁵ In brief, the EI measures epileptogenicity based on both: (i) the energy ratio between high frequencies (12–127 Hz) and low-frequency bands (4–12 Hz), (ii) the delay of this abrupt change from low to high frequencies in a given structure relative to the first structure, involved by the fast discharge. The cEI combines the original EI and a directed functional connectivity measure (“out-degree”) in a single quantity. The cEI was

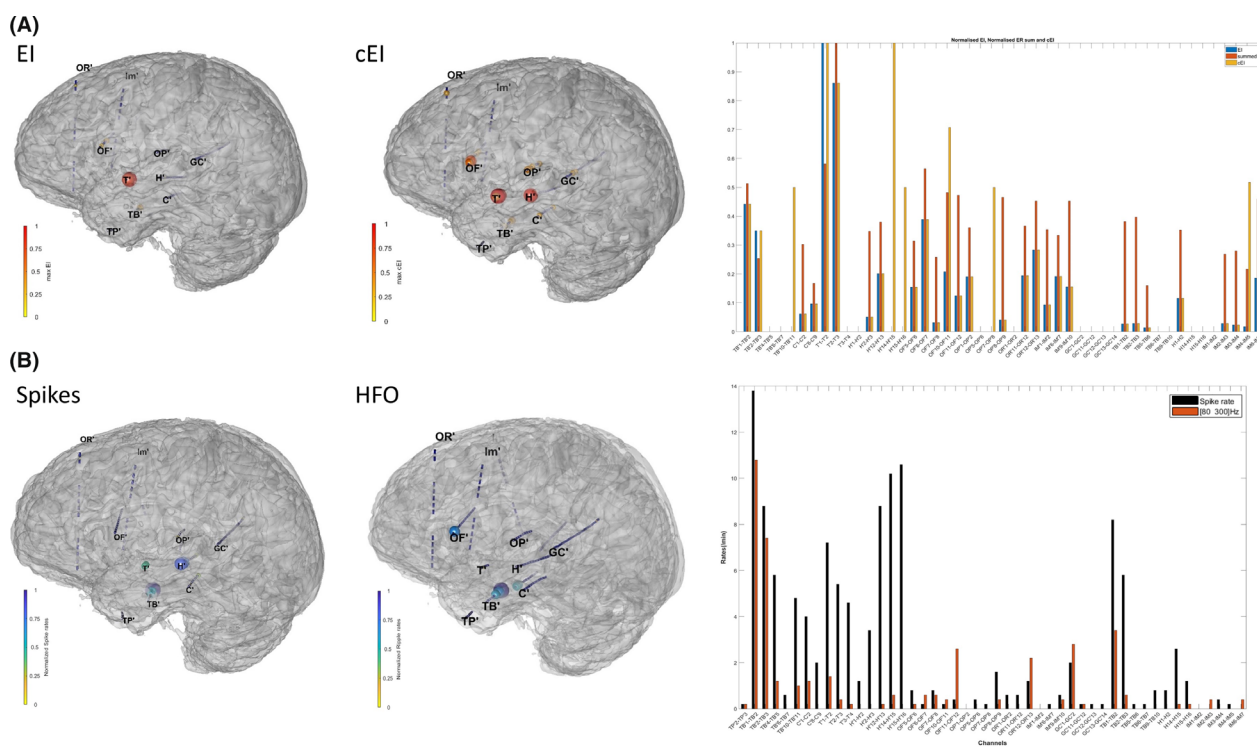


Figure 1. Example of the epileptogenic zone quantification using ictal and interictal epileptogenicity markers. Quantified ictal and interictal stereoelectroencephalography (SEEG) data of a patient suffering from drug-resistant epilepsy associated with a left temporal lateral ganglioglioma are shown. The epileptogenic zone (EZ) defined by visual analysis included the left anterior T1 (perilesional cortex sampled by the electrode T', just posteriorly to the lesion) up to Heschl gyrus, the temporal pole, the amygdala, and the anterior hippocampus. The resection of these structures sparing the hippocampus led to seizure freedom (Engel class I). (A) Ictal markers. The maximal Epileptogenicity Index (EI,¹⁵ left panel) and Connectivity EI (cEI,²⁰ middle panel) values quantified from two spontaneous seizures are represented as spheres on the patient's 3D brain mesh with implanted electrodes. Right panel: Graph showing epileptogenicity values quantified for each contact within the gray matter using EI (blue) and cEI (yellow); EI energy ratio is shown in red. The EZ defined by EI (EI ≥ 0.41) includes the left anterior T1 (T'1-3) and the left anterior hippocampus (TB'1-2). The EZ defined by cEI (cEI ≥ 0.65) includes the left anterior T1 (T'1-3) and the left posterior T1 with adjacent superior temporal sulcus (H'14-16). B. Interictal markers. Left and middle panels: the maximal normalized Spike- and high-frequency oscillations HFO (HFO, 80–300 Hz) rates quantified using Delphos detector³⁸ are shown on the patient's 3D brain mesh. Right panel: Graph showing the spike- (black) and the ripple (orange) rates/min quantified for each contact from a 5-min period of NREM sleep. The EZ defined by Spikes (Spikes ≥ 0.48) includes the left anterior T1 (T'1-4), the left posterior T1 and superior temporal sulcus (H'12-16), the left anterior hippocampus (TB'1-3) and the right rhinal cortex (TB1-2). The EZ defined by HFO (HFO ≥ 0.38) includes the left anterior hippocampus, the left anterior T2 (TB'10-11), the left F3 pars opercularis (OF'11-12) and the right rhinal cortex (TB1-2).

computed as described in Balatskaya et al.,²⁰ while employing the linear regression coefficient r^2 instead of the nonlinear regression coefficient h^2 to calculate the out-degree. This allowed a greater speed of calculation with comparable performances. In each patient and for each bipolar channel, the maximal normalized EI and the maximal cEI values from all the analyzed seizures were computed.

Interictal epileptogenicity markers (Fig. 1B), spikes, and HFO (80–300 Hz) were automatically quantified using Delphos (Detector of Electrophysiological Oscillations and Spikes)³⁸ on three 5-min periods of awake resting state and three 5-min periods of non-rapid eye movement (NREM) sleep recordings (48 h after the implantation, at least 2 h after a seizure)^{23,24} sampled at 1024 Hz. The respective interictal periods were selected by visual analysis from two contiguous 1-hour blocs of night sleep and from two contiguous 1-hour blocs of the resting state recordings, respectively, to account for possible fast-ultradian fluctuations of interictal activities. The selection criteria were the good-quality recording (least or no artifacts) and the presence of visually observed interictal epileptic activity (spikes, sharp-waves, low-voltage polyspikes- and fast activities). For each channel, the maximal normalized rate per minute for each marker was computed from a total of six 5-min datasets corresponding to 30 min of interictal recordings. We also quantified a combined measure, Spikes \times HFO, which corresponds to the geometric mean of the spike and HFO rate obtained by calculating the square root of the product of the two rates: Spikes \times HFO = $\sqrt{\text{spike rate} \times \text{HFO rate}}$.

Finally, two measures combining the interictal and ictal markers were quantified: Spikes \times EI and Spikes \times cEI, each obtained by calculating the square root of the product of the normalized spike rates and the normalized EI or cEI values, respectively; Spike \times EI = $\sqrt{\text{spike rate} \times \text{EI}}$; Spike \times cEI = $\sqrt{\text{spike rate} \times \text{cEI}}$.

ROI definition

The bipolar SEEG contacts within the gray matter were used as regions of interest (ROI) to assess the performances of different biomarkers and study the correlation between the EZ resection rate and surgical prognosis as well as between the EZ extent and surgical prognosis. The EZ hypothesis established by the consensus of two expert clinicians (FB, JM) based on visual analysis of SEEG data¹⁰ was used as clinically defined EZ (EZc). The EZc was defined according to the French guidelines on SEEG³⁴ as the brain regions primarily involved in seizure genesis, by visual inspection of ictal (spontaneous and stimulated seizures) and interictal SEEG recordings. Seizure onset was defined as the first change of SEEG

signal within the context of a sustained rhythmic discharge and subsequent appearance of clinical signs.¹⁰ The presence of a distinct seizure-onset pattern, the dynamics and spatial extension of ictal discharge, as well as the presence and morphology of interictal epileptiform discharges and of background alteration on the respective channels were assessed. The discrepancies in interpretation were solved through the collegial decision between the clinical experts.

For each epileptogenicity marker, a threshold has been established (see [Statistical analysis](#)) above which the respective contact was defined as belonging to the quantified EZ (EZq). Following thresholds were determined: EI ≥ 0.41 ; cEI ≥ 0.65 ; Spikes ≥ 0.48 ; HFO ≥ 0.38 ; Spikes \times HFO ≥ 0.38 ; Spikes \times EI ≥ 0.32 ; Spikes \times cEI ≥ 0.44 . All ROI were labeled according to their status as EZc or non-EZc and as EZq or non-EZq for each marker. The resected contacts were defined using GARDEL software. In brief, the co-registration of the postimplantation CT with electrodes with the postoperative MRI, and that of the post- and preoperative MRI were performed; resected contacts were identified by visual inspection (SMV, TM, JS). For all ROI, a “resected” or “non-resected” status was assigned.

Statistical analysis

Statistical analyses were performed using Matlab statistics toolbox (15.0 and 18.0). As we are facing an imbalanced problem (much more non-EZ than EZ contacts), we decided to use precision and recall measures.³⁹ While precision—also called positive predicted value—is the proportion of correct predictions among all the positive class predictions, recall—also called sensitivity—gives the proportion of correct predictions among the true-positive values.

$$\text{precision} = \frac{\text{True Positive}}{\text{True Positive} + \text{False Positive}}$$

$$\text{recall} = \frac{\text{True Positive}}{\text{True Positive} + \text{False Negative}}$$

A way to summarize precision and recall is to compute F_β which is the weighted harmonic mean between these two metrics.

$$F_\beta = \frac{(1 + \beta^2) \times \text{precision} \times \text{recall}}{(\beta^2 \times \text{precision}) + \text{recall}}$$

We chose $\beta = 0.5$ to give more weight to precision than recall. A $F_{0.5}$ score close to 1 highlights a good coherence between the classification based on a given marker and our reference, the clinically defined EZ (EZc). The optimal threshold for each marker was that corresponding to the highest $F_{0.5}$ in each of the 32 seizure-free

patients (Engel class I). Precision recall was then used to compare the EZ_q defined by different markers using the established thresholds against the clinically defined EZ (EZ_c). We assessed the performances of different markers (i) in the whole cohort of 53 patients; (ii) according to surgical outcome (seizure-free vs. not seizure-free patients); (iii) according to the presence or not of an intrinsically epileptogenic lesion (cases with histologically confirmed focal cortical dysplasia, hippocampal sclerosis, dysembryoplastic neuroepithelial tumor (DNET), ganglioglioma, tuberous sclerosis versus cases with gliotic scar or no lesion, which common feature is the absence of an intrinsically epileptogenic lesion).

The Kolmogorov–Smirnov test was used to assess the normality of the distribution. As the data were not normally distributed, two-sided Wilcoxon test was used to assess group differences in the EZ resection rates (percentage of resected EZ_c or EZ_q) between the seizure-free and not seizure-free patients. Correlation between the EZ resection rates and surgical prognosis according to Engel class was assessed using Spearman test. Correlations between the EZ extent (number of EZ contacts) and surgical outcome (seizure-free vs. not seizure-free) were investigated using Wilcoxon test. A *P*-value <0.05 was considered as significant.

A logistic regression was performed to assess the relevance of the number of EZ contacts according to each quantitative marker: EI, cEI, Spikes, HFO, Spikes × HFO, Spikes × EI, Spikes × cEI, as well as of clinical variables (age at onset, epilepsy duration, normal MRI, epilepsy type, histology) for predicting surgical outcome (seizure-free or not seizure-free). We simplified the logistic model using feature selection based on Akaike Information Criteria (function step AIC of the MASS package in R).

Results

Patients' clinical characteristics

Patients' clinical data are summarized in Table 1. Fifty-three patients (21 males, 32 females) were included. Mean age at epilepsy onset was 14.2 years (range 0.1–55; childhood onset in 68%), mean duration of epilepsy was 14.5 years (range 2.5–54), mean age at evaluation: 28.9 years (range 4–70). An MRI-visible lesion was present in 64% of cases. The EZ topography was temporal in 26 cases, frontal in 13 cases, parietal in 2, occipital in 2, and multilobar in 10 cases. The most common surgical procedures were tailored resections, performed in 28 patients, followed by anterior temporal lobectomy in 20, disconnection in 3, and selective amygdalohippocampectomy in 2. The postsurgical outcome was favorable in 38 patients (Engel class I, 59%, Engel class II,

Table 1. Clinical characteristics of the patients.

Sex, male/female	21/32
Age at epilepsy onset, years	14.2 ± 13.2 (0.1–55)
Age at SEEG, years	28.9 ± 16.8 (4–70)
Epilepsy duration, years	14.5 ± 11.7 (2.5–54)
Side, left/right	30/23
MRI, normal/lesion, % (<i>n</i>)	36% (19)/64% (34)
Localization of the epileptogenic zone (<i>n</i>)	
Temporal	26
Frontal	13
Posterior	4
Multilobar	10
Surgery (<i>n</i>)	
Tailored resection	28
ATL	20
SAHE	2
Disconnection	3
Outcome (Engel class)	
I, % (<i>n</i>)	59% (31)
II, % (<i>n</i>)	13% (7)
III, % (<i>n</i>)	17% (9)
IV, % (<i>n</i>)	11% (6)
Histopathology (<i>n</i>)	
FCD	16
Hippocampal sclerosis	8
DNET	4
Ganglioglioma	1
Tuberous sclerosis	1
Glial scar	4
No lesion	15

Note: Data are presented as mean ± SD (range) or % (*n*).

Abbreviations: ATL, anterior temporal lobectomy; DNET, dysembryoplastic neuroepithelial tumor; FCD, focal cortical dysplasia; HS, hippocampal sclerosis; SAHE, selective amygdalohippocampectomy; SEEG, stereoelectroencephalography.

13%), with worthwhile improvement in 9 (Engel class III, 17%), and without significant improvement in 6 cases (Engel class IV, 11%). Histopathological findings comprised focal cortical dysplasia (FCD) in 16 cases, hippocampal sclerosis in 8, DNET in 4, ganglioglioma in 1, glial scar in 4, and tuberous sclerosis complex in 1. No specific lesion could be identified in 15 cases.

Performances of SEEG biomarkers as compared to clinical gold standard

We compared the ROI identified as epileptogenic by different SEEG biomarkers (EZ_q) against the EZ_c by using precision-recall. The results of the whole cohort of 53 patients are shown in Fig. 2. The Spikes × EI and the EI demonstrated the highest precision (0.74 and 0.70, respectively, Fig. 2A), followed by the Spikes × cEI (0.65) and the cEI (0.59), whereas interictal biomarkers showed lower precision against EZ_c (Spikes, 0.48; HFO [80–300 Hz], 0.29; Spikes × HFO, 0.42). The recall (Fig. 2B)

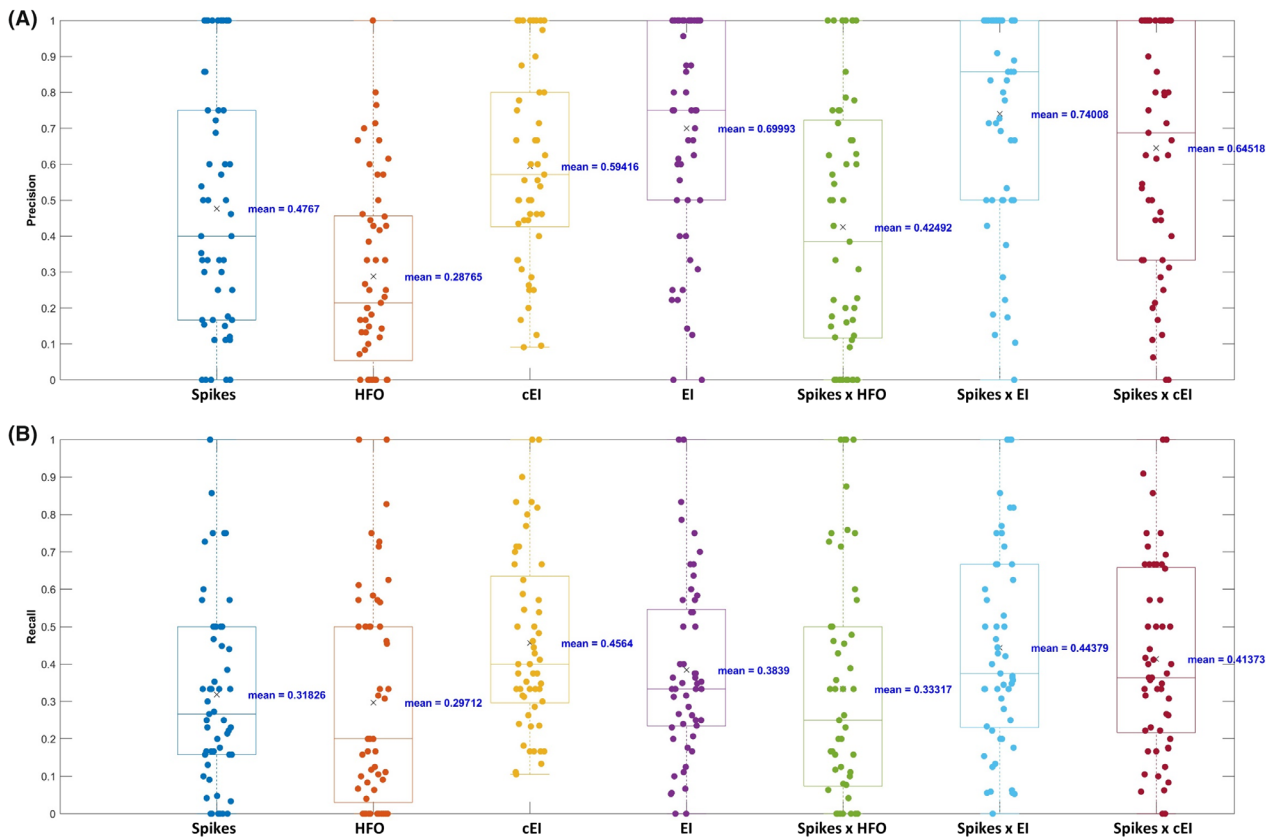


Figure 2. Performances of SEEG biomarkers as compared to clinical gold standard. Precision (A) and Recall (B) for the quantified EZ using Spikes, HFO, cEI, EI, Spikes \times HFO, Spikes \times EI, and Spikes \times cEI versus clinically defined EZ in the whole cohort of 53 operated patients. Spikes \times EI showed the best precision against the clinical analysis. The cEI and spike \times EI demonstrated the best sensitivity.

was comparable for the cEI (0.46) and the combined ictal–interictal biomarkers (Spikes \times EI, 0.44; Spikes \times cEI, 0.41). It was slightly inferior for the EI (0.38), while the Spikes (0.32), HFO (0.30) and Spikes \times HFO (0.33) showed low recall against the EZc. Regarding the presence or absence of an epileptogenic lesion, we compared a subgroup of patients ($n = 30$) with intrinsically epileptogenic lesions, including histologically confirmed focal cortical dysplasia, hippocampal sclerosis, dysembryoplastic neuroepithelial tumor (DNET), ganglioglioma, and tuberous sclerosis, with a subgroup of patients ($n = 23$) without intrinsically epileptogenic lesions, including gliotic scar or no lesion. The precision of the ictal and combined ictal–interictal biomarkers did not differ significantly between these groups and remained identical or comparable to that of the whole cohort. We observed the highest precision of the Spikes \times EI (0.74 in both groups) and the EI (0.69 in the group with an epileptogenic lesion vs. 0.72 in the group without epileptogenic lesion) followed by the Spikes \times cEI (0.71 vs. 0.57) and the cEI (0.62 vs. 0.55). The same situation was observed for the HFO (0.30 vs.

0.27 for the groups with and without epileptogenic lesion, respectively) and Spikes \times HFO (0.42 vs. 0.44). The precision of the Spikes was significantly better in the group with an epileptogenic lesion (0.56) compared to the group without epileptogenic lesion (0.37, $P < 0.05$, Wilcoxon), but still inferior to the precision of the ictal markers within each respective group. The recall remained comparable to that of the whole cohort across these two groups for all the assessed biomarkers. It did not differ significantly depending on the presence or not of an epileptogenic lesion for the ictal markers (cEI, 0.47 vs. 0.43; EI, 0.38 vs. 0.39) and the Spikes \times EI (0.46 vs. 0.42). The recall tended to improve in the presence of an epileptogenic lesion, although not reaching statistical significance, for the Spikes \times cEI (0.47 vs. 0.34, $P = 0.051$, Wilcoxon) and the interictal markers (Spikes, 0.36 vs. 0.26, $P = 0.054$; HFO, 0.34 vs. 0.24, $P = 0.30$; Spikes \times HFO, 0.37 vs. 0.28, $P = 0.27$, Wilcoxon). When comparing the performances separately in the seizure-free and not seizure-free patient groups, all the evaluated biomarkers showed better precision in seizure-free compared to not seizure-free patients. This difference in precision

according to the outcome tended to be significant for the cEI (0.65 vs. 0.50, $P = 0.053$) and the Spikes \times EI (0.80 vs. 0.64, $P = 0.068$). The recall did not differ between the seizure-free and not seizure-free patients.

Correlation between the EZ resection rate and surgical prognosis

The extent of the EZ resection tended to be greater in seizure-free patients than in not seizure-free patients, both for the visually defined EZ and for the EZ quantified using ictal or combined ictal–interictal biomarkers (Fig. 3). Of note, the mean EZ resection ratio in seizure-free patients was 74% for the EZc and was varying between 58% and 67% for the EZq using ictal or

combined biomarkers, whereas in not seizure-free patients, the resection ratio was close to 60% for the EZc but did not exceed 47% for the EZq. A statistically significant difference in the EZ resection rate between the seizure-free and not seizure-free patients was only present for the EZq defined by EI (59% vs. 33%, $P < 0.01$) or cEI (58% vs. 38%, $P = 0.02$) but not for the clinically defined EZ (EZc) (74% vs. 58%, $P = 0.098$). The same trend was demonstrated for the resection rates of the EZq defined by combined ictal–interictal markers (Spikes \times EI, 66% vs. 45%, $P = 0.05$; Spikes \times cEI, 67% vs. 47%, $P = 0.08$). Conversely, there was no difference in the extent of the EZ resection between the seizure-free and not seizure-free groups when the EZq was defined by interictal markers (Spikes, 54% vs. 48%, $P = 0.56$; HFO, 45% vs. 43%, $P = 0.78$).

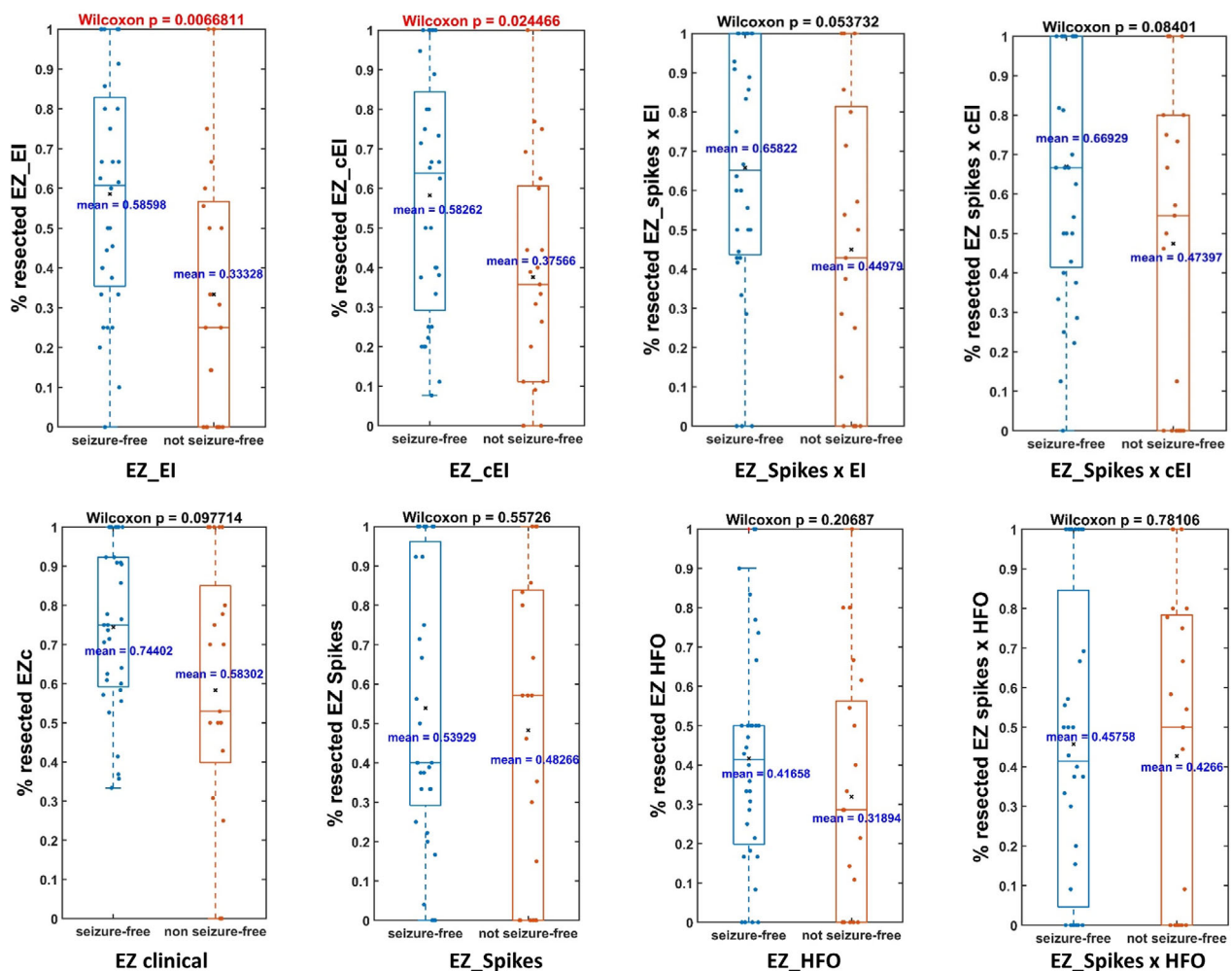


Figure 3. The extent of EZ resection in seizure-free versus non-seizure-free patients. Percentage of resected epileptogenic contacts as defined by ictal (EZ_EI; EZ_cEI), interictal (EZ_Spikes, EZ_HFO, EZ_spikes \times HFO), and combined ictal–interictal (EZ_spikes \times EI, EZ_spikes \times cEI) markers as well as by visual analysis (EZc) comparing the seizure-free and the non-seizure-free group. The EZ resection rates were significantly higher in seizure-free than in non-seizure-free patients for the EZ quantified by ictal markers; the same trend was present for the combined markers and the EZc, while the resection rates of EZ quantified using interictal markers did not differ depending on surgical outcome.

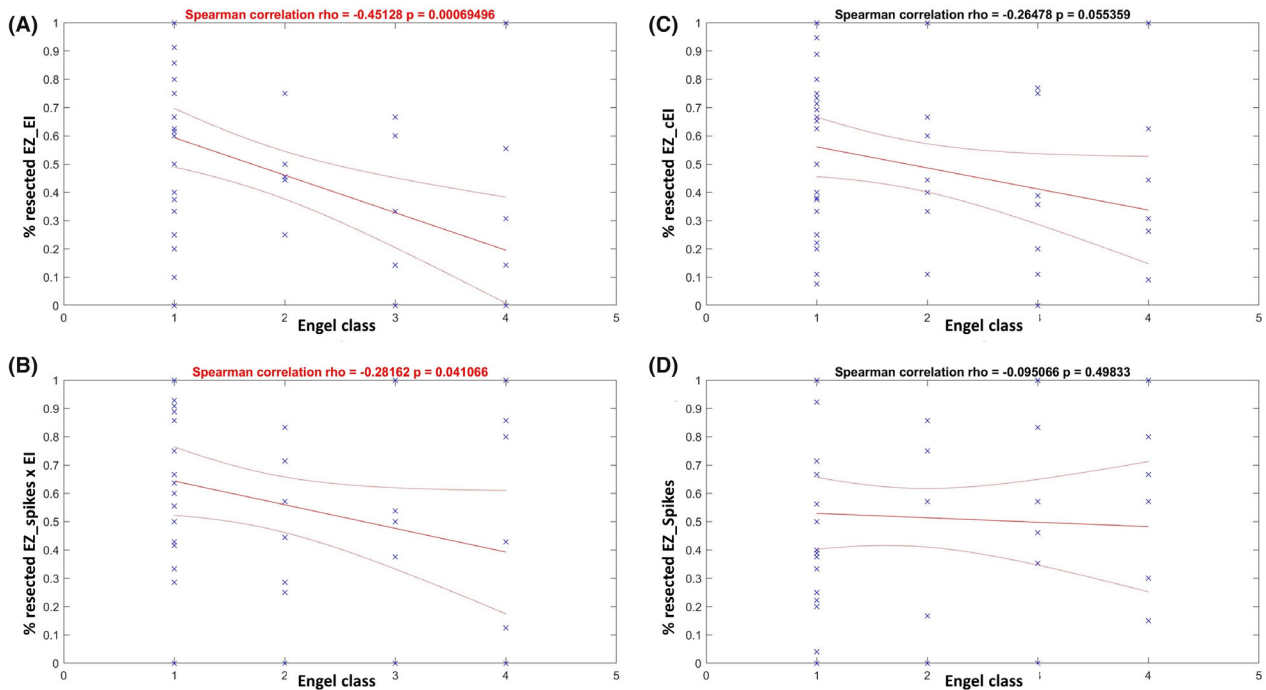


Figure 4. Correlation between the EZ resection rate and surgical prognosis according to Engel class. The EZ resection rate was significantly correlated with prognosis according to Engel class for the EZ quantified using EI (A) and Spikes \times EI (B). The same trend was observed for the EZ quantified by cEI (C) but not for the EZ quantified by spikes (D), nor for the HFO or visual analysis (not shown).

42% vs. 32%, $P = 0.21$; Spikes \times HFO 46% vs. 43%, $P = 0.78$).

Furthermore, the EZ resection rates were significantly correlated with prognosis according to Engel class (better prognosis being associated with a higher percentage of resected EZ contacts) for the EZ quantified by EI ($P < 0.001$, $\rho = -0.45$, Spearman, Fig. 4A) and by Spikes \times EI ($P = 0.04$, $\rho = -0.28$, Fig. 4B). This correlation tended to be significant for cEI ($P = 0.055$, $\rho = -0.26$, Fig. 4C), whereas no correlation was demonstrated for the EZc or the EZq defined by Spikes ($P = 0.49$, $\rho = -0.095$, Fig. 4D), HFO, or Spikes \times HFO.

Correlation between the EZ extent and surgical prognosis

For the EZc and EZq defined by different biomarkers, the number of EZ contacts did not significantly differ between the seizure-free and not seizure-free patients (Wilcoxon, $P > 0.05$). The multivariate analysis using the AIC-optimized logistic regression model for predicting surgical outcome included epilepsy duration, normal MRI, the number of EZq contacts according to Spikes and according to Spikes \times EI, respectively. Results showed no statistically significant features even though

the model had reliable goodness of fit to the data ($\chi^2 = 8.63$, P -value = 0.374).

Discussion

The optimal definition of the epileptogenic zone remains a major goal in the interpretation of SEEG.¹⁰ To this end, the search for quantified markers of epileptogenicity based on computational methods^{11,12} has increased in the last fifteen years. These studies report model-free and model-based approaches including ictal and interictal epileptogenicity markers,^{15,17,20,23,28,40,41} structural^{42–44} and functional connectivity,⁴⁵ graph measures,⁴⁶ and individualized large-scale brain modeling.^{35,47,48} Taken together, they provided a large body of evidence that successful surgical outcomes depend on the proper characterization of the seizure-generating network. Despite its increasing development, SEEG quantification is rarely used routinely in most epilepsy surgery centers, probably due to its uncertain added value and practical difficulties of use.

This study is the first to evaluate the performances of ictal (EI, cEI), interictal (spikes, HFO [80–300 Hz], spikes \times HFO), and combined ictal–interictal (spikes \times EI, spikes \times cEI) epileptogenicity markers in predicting surgical outcome compared to the clinical gold standard in a representative cohort of 53 children and

adults who underwent epilepsy surgery following SEEG. All the SEEG markers tested herein are easily applicable during a routine presurgical work-up, particularly thanks to the open-source software available.

First, we evaluated the performances of quantified markers in detecting the epileptogenic contacts identified by clinicians. Whereas the EI showed better precision than the cEI (0.70 vs. 0.59), the latter showed better recall compared to the EI (0.46 vs. 0.38) and other markers. In other words, the cEI is more sensitive but has a slightly lower positive predictive value than the EI in detecting the EZ. However, precision is likely more pertinent when using SEEG-signal quantification in a routine clinical setting, as it helps to discriminate the EZ. Importantly, combining each of these ictal markers with interictal spikes further improved the detection accuracy, with Spikes \times EI showing the highest precision among all markers tested, both in the whole cohort (0.74) and in the sub-cohort of seizure-free patients (0.80), closely followed by the EI and Spikes \times cEI. For the cEI and Spikes \times EI, the concordance with the EZc was higher in seizure-free than in not seizure-free patients, suggesting that in the latter group, these markers could identify some epileptogenic regions eventually missed by visual analysis. Ictal and combined ictal–interictal markers outperformed the classical interictal markers (Spikes, HFO 80–300 Hz) showing low precision (0.48, 0.29) and recall (0.32, 0.30) against the EZc. Furthermore, while the performances of spikes varied significantly depending on the presence or absence of an epileptogenic lesion, with significantly higher precision in the lesional cases, the performances of the ictal markers and of the Spikes \times EI remained stable, with equally high precision in both conditions, indicating that these markers were as effective in localizing likely less focal (gliotic scars and no lesions) compared to the well outlined lesional cases (FCD, hippocampal sclerosis, DNET, ganglioglioma). Combining the two interictal markers in a single measure, Spikes \times HFO did not improve detection accuracy. This result does not confirm the result of our previous study, based on a smaller patient cohort, showing better performances of the Spikes \times HFO compared to other interictal markers,²⁴ probably due to higher sampling rates allowing better detection of fast ripples. However, our actual result is in agreement with a recent study by Thomas et al.⁴¹ evaluating different interictal biomarkers to discriminate the EZ in seizure-free and not seizure-free patients and showing that combining multiple features did not improve the classification performances. Conversely, it has been previously demonstrated that the occurrence of gamma activity preceding interictal epileptiform discharges was associated with the seizure onset zone.⁴⁹ In line with these findings, the latter study showed that the spike-gamma rate in wakefulness

outperformed the visually defined seizure onset zone, the ripple rate as well as the geometric mean of spikes and HFOs for classification of surgical outcome.

Second, we found a statistically significant relation between the EZ resection rate and surgical prognosis (higher in seizure-free than in not seizure-free and higher in patients with better seizure outcome) for the EZq defined by ictal SEEG markers or Spikes \times EI but not for the clinically defined EZ. This result may explain the quite paradoxical result of a recent study on a pediatric SEEG cohort, in which the percentage of resected EZ contacts defined by visual analysis was not associated with seizure freedom.⁵⁰ Other studies have shown higher epileptogenicity values or higher numbers of non-resected epileptogenic regions quantified using gamma index²⁸ or virtual epileptic patient (VEP)³⁵ in not seizure-free compared to seizure-free patients. A more accurate definition of epileptogenic tissue can thus be obtained using these ictal biomarkers. In our hands, the resection rates of EZ quantified using interictal markers (spikes, HFO, or Spikes \times HFO) did not differ depending on surgical outcome indicating a less informative role for these biomarkers. In line with our findings, a recent prospective multicenter study by Jacobs et al.²³ have shown that individual prognostication of surgery outcome based on removing interictal HFO was true in only 67% of patients. Nonetheless, the performances of interictal biomarkers may be improved by combination with other features, as demonstrated for the above-mentioned spikes with preceding gamma activity⁴¹ or fast ripples network graph theoretical measures.⁵¹

Regarding other potential determinants of prognosis, in the present study, the number of epileptogenic contacts defined by ictal, interictal, or combined markers was not correlated to surgical outcome suggesting that a higher extent of the EZN was not associated with a lower chance for surgical success. Furthermore, no possible cofounders of seizure freedom could be identified among the clinical variables tested including age at onset, epilepsy duration, normal MRI, epilepsy type, and histology.

Finally, according to our data, the resection of at least 58% of the EZ using ictal and of at least 66% of the EZ using combined ictal–interictal markers is required to achieve seizure freedom in most patients. This allows to assume that the complete EZ resection is not mandatory to control seizures, suggesting that a relatively focal resection or disconnection is likely to impact the whole EZN. This effect could be due to the connectivity changes induced by surgery but also to the removal of the most epileptogenic and/or connected nodes, given the intra- and interregional variability of the epileptogenicity values within the EZN. Regarding clinical decision-making, the quantification using ictal biomarkers with validated

thresholds has significant advantages for the epilepsy surgery team. First, it objectively identifies the regions that belong to the EZN, which should be targeted for removal or disconnection through surgery. Second, by providing information on the epileptogenicity level of various nodes within the EZN, the quantification can assist in estimating the risk/benefit ratio of complete resection in relation to functional constraints, and ultimately choose an alternative surgical plan that focuses on the most epileptogenic nodes. *In silico* surgery modeling have shown that the resection of some crucial nodes may be sufficient for effective results.⁵² Different surgical scenarios could be tested using the repertoire of virtual surgery approaches,⁵³ which clinical translation is ongoing,⁴⁸ to define at the individual level, the minimum number of EZ regions to resect to achieve seizure control, while offering the best functional outcome. Last but not the least, the epileptogenicity values of each explored structure can be easily visualized within the patient's anatomy using an open-source EpiTools software suite,³⁷ offering a concise and realistic 3D image of the EZN for surgical decision and intervention planning.

Limitations

Some bias and potential limitations should be mentioned. First, there is bias due to the retrospective study design and selection of patients undergoing curative surgery, while patients contraindicated for surgery following SEEG or became seizure-free after SEEG-thermocoagulation were not included. It is important to note that the present study had a limited number of patients and was conducted in a single center. Therefore, to draw a definitive conclusion on the generalizability of the data, larger multicenter studies would be necessary. As a further limitation, due to the lack of interictal datasets with sampling >1024 Hz for the majority of included patients, the HFO analysis was limited to the oscillations in the ripple band, some of them might account for the physiological HFO, while the fast ripples could not be properly evaluated. Normalizing the HFO rates according to the regional variances²⁶ could improve specificity. Regarding the spikes quantification, although several interictal SEEG segments were used per patient, both from wakefulness and from NREM sleep, temporal fluctuations in spike rates and spatial distribution represent a bias, which might be better taken into account, for example, by detection on prolonged recordings.^{33,54} Such fluctuations have been also demonstrated for the HFO.⁵⁵ Moreover, the fast-ultradian dynamics of the rate of interictal epileptiform discharges (IED), may impair the precision of EZ identification, as could be demonstrated in a recent study by our group,⁵⁶ also showing that the minimization of the rate of

interictal events across all the SEEG channels is a good predictor of the interictal epoch for near-optimal EZ localization based on specific IED subtypes. The use of the spike-gamma metrics recently proposed by Thomas et al.⁴¹ could also be interesting. Finally, the sampling problem is a well-known bias for all SEEG-based quantification methods. Consequently, there is also limitation due to the choice of the SEEG contacts as the ROI, since there might be a bias due to a possible oversampling of the EZ. The use of personalized virtual brain models such as virtual epileptic patient⁴⁸ is a promising complementary approach to overcome this limitation.³⁵

Conclusion

Epileptogenic zone quantification offers real advantages for facilitating SEEG interpretation and predicting surgical outcome. Ictal (EI, cEI) or combined ictal-interictal (Spikes \times EI, Spikes \times cEI) SEEG markers overperformed the classical interictal markers (Spikes, HFO, Spikes \times HFO), both for detecting the EZ and predicting the seizure freedom. Combining ictal and interictal markers in a single measure improved detection accuracy. Spikes \times EI showed the best precision against the clinical analysis. The resection rate of the EZ defined by ictal markers and by Spikes \times EI significantly correlated with surgical prognosis. However, complete EZ resection was not mandatory to control seizures.

Acknowledgments

Authors thank Prof Agnes Trebuchon, Dr Francesca Bonini, Dr Aileen McGonigal, Dr Francesca Pizzo, Dr Nathalie Villeneuve, Dr Lisa Vaugier for clinical management of included patients.

Conflicts of Interest

The authors have no conflicts of interest to disclose.

Funding Information

This work is funded through the French National Research Agency (ANR) as part of the second "Investissements d'Avenir" program (ANR-17-RHUS-0004, EPINOV).

Author Contributions

Julia Makhalova: conception and design of the study, acquisition, and analysis of data, drafting the manuscript and figures. Tanguy Madec: design of the study, acquisition, and analysis of data, drafting the manuscript.

Samuel Medina Villalon: software; statistical analysis, drafting the manuscript and figures. Aude Jegou: software; database construction and analysis of data. Stanislas Lagarde: acquisition of data, review, and editing of the manuscript. Romain Carron: performed stereoelectroencephalography, review, and editing of the manuscript. Didier Scavarda: performed stereoelectroencephalography and epilepsy surgery, review and editing of the manuscript. Elodie Garnier: statistical analysis, review, and editing of the manuscript. Christian G. Bénar: data analysis, review, and editing of the manuscript. Fabrice Bartolomei: conception and design of the study, acquisition, and analysis of data, drafting the manuscript and figures.

References

- Jehi L, Friedman D, Carlson C, et al. The evolution of epilepsy surgery between 1991 and 2011 in nine major epilepsy centers across the United States, Germany, and Australia. *Epilepsia*. 2015;56(10):1526-1533. Accessed January 13, 2022. <https://pubmed.ncbi.nlm.nih.gov/26250432/>
- Cardinale F, Rizzi M, Vignati E, et al. Stereoelectroencephalography: retrospective analysis of 742 procedures in a single centre. *Brain*. 2019;142(9):2688-2704. Accessed December 13, 2021. <https://pubmed.ncbi.nlm.nih.gov/31305885/>
- Lagarde S, Buzori S, Trebuchon A, et al. The repertoire of seizure onset patterns in human focal epilepsies: determinants and prognostic values. *Epilepsia*. 2019;60(1):85-95. Accessed December 13, 2021. <https://pubmed.ncbi.nlm.nih.gov/30426477/>
- Bartolomei F, Cosandier-Rimele D, McGonigal A, et al. From mesial temporal lobe to temporoparietal seizures: a quantified study of temporal lobe seizure networks. *Epilepsia*. 2010;51(10):2147-2158. Accessed December 19, 2022. <https://pubmed.ncbi.nlm.nih.gov/20738379/>
- Bartolomei F, Lagarde S, Wendling F, et al. Defining epileptogenic networks: contribution of SEEG and signal analysis. *Epilepsia*. 2017;58(7):1131-1147. doi:10.1111/epi.13791
- Spencer SS. Neural networks in human epilepsy: evidence of and implications for treatment. *Epilepsia*. 2002;43(3):219-227. doi:10.1046/j.1528-1157.2002.26901.x
- Ryvlin P, Cross JH, Rheims S. Epilepsy surgery in children and adults. *Lancet Neurol*. 2014;13(11):1114-1126. Accessed September 1, 2022. <https://pubmed.ncbi.nlm.nih.gov/25316018/>
- Lamberink HJ, Otte WM, Blümcke I, et al. Seizure outcome and use of antiepileptic drugs after epilepsy surgery according to histopathological diagnosis: a retrospective multicentre cohort study. *Lancet Neurol*. 2020;19(9):748-757. Accessed January 16, 2023. <https://pubmed.ncbi.nlm.nih.gov/32822635/>
- Jehi L, Jette N, Kwon C, et al. Timing of referral to evaluate for epilepsy surgery: expert consensus recommendations from the surgical therapies commission of the International League Against Epilepsy. *Epilepsia*. 2022;63:2491-2506. Accessed September 1, 2022. <https://pubmed.ncbi.nlm.nih.gov/35842919/>
- Bartolomei F, Nica A, Valenti-Hirsch MP, Adam C, Denuelle M. Interpretation of SEEG recordings. *Neurophysiol Clin*. 2018;48(1):53-57.
- Jobst BC, Bartolomei F, Diehl B, et al. Intracranial EEG in the 21st century. *Epilepsy Curr*. 2020;20(4):180-188. Accessed March 27, 2023. <https://pubmed.ncbi.nlm.nih.gov/32677484/>
- Bernabei JM, Li A, Revell AY, et al. Quantitative approaches to guide epilepsy surgery from intracranial EEG. *Brain*. 2023;139(4):16-17. Accessed February 1, 2023. <https://pubmed.ncbi.nlm.nih.gov/36623936/>
- Frauscher B, Bartolomei F, Kobayashi K, et al. High-frequency oscillations: the state of clinical research. *Epilepsia*. 2017;58(8):1316-1329. Accessed September 1, 2022. <https://pubmed.ncbi.nlm.nih.gov/28666056/>
- Wendling F, Bartolomei F, Mina F, et al. Interictal spikes, fast ripples and seizures in partial epilepsies—combining multi-level computational models with experimental data. *Eur J Neurosci*. 2012;36(2):2164-2177. Accessed December 19, 2022. <https://pubmed.ncbi.nlm.nih.gov/22805062/>
- Bartolomei F, Chauvel P, Wendling F. Epileptogenicity of brain structures in human temporal lobe epilepsy: a quantified study from intracerebral EEG. *Brain*. 2008;131(7):1818-1830.
- David O, Blauwblomme T, Job A-S, et al. Imaging the seizure onset zone with stereo-electroencephalography. *Brain*. 2011;134:2898-2911. Accessed July 12, 2021. <https://academic.oup.com/brain/article/134/10/2898/323878>
- Grinenko O, Li J, Mosher JC, et al. A fingerprint of the epileptogenic zone in human epilepsies. *Brain*. 2018;141(1):117-131. Accessed December 24, 2021. <https://pubmed.ncbi.nlm.nih.gov/29253102/>
- Gnatkovsky V, De Curtis M, Pastori C, et al. Biomarkers of epileptogenic zone defined by quantified stereo-EEG analysis. *Epilepsia*. 2014;55(2):296-305. Accessed December 24, 2021. <https://pubmed.ncbi.nlm.nih.gov/24417731/>
- Gnatkovsky V, Pelliccia V, de Curtis M, Tassi L. Two main focal seizure patterns revealed by intracerebral electroencephalographic biomarker analysis. *Epilepsia*. 2019;60(1):96-106. Accessed July 10, 2023. <https://pubmed.ncbi.nlm.nih.gov/30565671/>
- Balatskaya A, Roehri N, Lagarde S, et al. The “Connectivity Epileptogenicity Index” (cEI), a method for mapping the different seizure onset patterns in StereoElectroEncephalography recorded seizures. *Clin Neurophysiol*. 2020;131(8):1947-1955. Accessed November 5, 2020. <https://pubmed.ncbi.nlm.nih.gov/32622336/>

21. Wendling F, Bartolomei F, Bellanger JJ, Chauvel P. Interpretation of interdependencies in epileptic signals using a macroscopic physiological model of the EEG. *Clin Neurophysiol.* 2001;112:1201-1218.
22. Jacobs J, Zijlmans M, Zemann R, et al. High-frequency electroencephalographic oscillations correlate with outcome of epilepsy surgery. *Ann Neurol.* 2010;67(2):209-220.
23. Jacobs J, Wu JY, Perucca P, et al. Removing high-frequency oscillations: a prospective multicenter study on seizure outcome. *Neurology.* 2018;91(11):e1040-e1052. Accessed September 1, 2022. <https://pubmed.ncbi.nlm.nih.gov/30120133/>
24. Roehri N, Pizzo F, Lagarde S, et al. High-frequency oscillations are not better biomarkers of epileptogenic tissues than spikes. *Ann Neurol.* 2018;83(1):84-97. Accessed November 26, 2019. <http://www.ncbi.nlm.nih.gov/pubmed/29244226>
25. Weiss SA, Staba RJ, Sharan A, et al. Accuracy of high-frequency oscillations recorded intraoperatively for classification of epileptogenic regions. *Sci Rep.* 2021;11(1):21388. Accessed January 16, 2023. <https://pubmed.ncbi.nlm.nih.gov/34725412/>
26. Frauscher B, von Ellenrieder N, Zemann R, et al. High-frequency oscillations in the normal human brain. *Ann Neurol.* 2018;84(3):374-385. Accessed January 16, 2023. <https://pubmed.ncbi.nlm.nih.gov/30051505/>
27. Aubert S, Wendling F, Regis J, et al. Local and remote epileptogenicity in focal cortical dysplasias and neurodevelopmental tumours. *Brain.* 2009;132(11):3072-3086. Accessed November 5, 2020. <https://pubmed.ncbi.nlm.nih.gov/19770216/>
28. Job AS, David O, Minotti L, Bartolomei F, Chabardès S, Kahane P. Epileptogenicity maps of intracerebral fast activities (60–100 Hz) at seizure onset in epilepsy surgery candidates. *Front Neurol.* 2019;10:1263. Accessed December 24, 2021. <https://pubmed.ncbi.nlm.nih.gov/34826646/>
29. Makhalova J, Le Troter A, Aubert-Conil S, et al. Epileptogenic networks in drug-resistant epilepsy with amygdala enlargement: assessment with stereo-EEG and 7 T MRI. *Clin. Neurophysiol.* 2021;133:94-103. Accessed December 10, 2021. <https://pubmed.ncbi.nlm.nih.gov/34826646/>
30. González Otárola KA, von Ellenrieder N, Cuello-Oderiz C, et al. High-frequency oscillation networks and surgical outcome in adult focal epilepsy. *Ann Neurol.* 2019;85(4):485-494. Accessed January 10, 2023. <https://pubmed.ncbi.nlm.nih.gov/30786048/>
31. Lagarde S, Roehri N, Lambert I, et al. Interictal stereotactic-EEG functional connectivity in refractory focal epilepsies. *Brain.* 2018;141(10):2966-2980.
32. Zweiphenning W, Klooster MA v t, van Klink NEC, et al. Intraoperative electrocorticography using high-frequency oscillations or spikes to tailor epilepsy surgery in the Netherlands (the HFO trial): a randomised, single-blind, adaptive non-inferiority trial. *Lancet Neurol.* 2022;21(11):982-993.
33. Klimes P, Peter-Derex L, Hall J, Dubeau F, Frauscher B. Spatio-temporal spike dynamics predict surgical outcome in adult focal epilepsy. *Clin Neurophysiol.* 2022;134:88-99.
34. Isnard J, Taussig D, Bartolomei F, et al. French guidelines on stereoelectroencephalography (SEEG). *Neurophysiol Clin.* 2018;48(1):5-13. Accessed November 26, 2019. <http://www.ncbi.nlm.nih.gov/pubmed/29277357>
35. Makhalova J, Medina Villalon S, Wang H, et al. Virtual epileptic patient brain modeling: relationships with seizure onset and surgical outcome. *Epilepsia.* 2022;63(8):1942-1955. Accessed September 1, 2022. <https://pubmed.ncbi.nlm.nih.gov/35604575/>
36. Colombet B, Woodman M, Badier JM, Bénar CG. AnyWave: a cross-platform and modular software for visualizing and processing electrophysiological signals. *J Neurosci Methods.* 2015;242:118-126.
37. Medina Villalon S, Paz R, Roehri N, et al. EpiTools, a software suite for presurgical brain mapping in epilepsy: intracerebral EEG. *J Neurosci Methods.* 2018;303:7-15. Accessed November 26, 2019. <https://linkinghub.elsevier.com/retrieve/pii/S0165027018300955>
38. Roehri N, Lina JM, Mosher JC, et al. Time-frequency strategies for increasing high frequency oscillation detectability in intracerebral EEG. *IEEE Trans Biomed Eng.* 2016;63(12):2595. Accessed January 30, 2023. <https://pubmed.ncbi.nlm.nih.gov/27134253/>
39. Juba B, Le HS. Precision-recall versus accuracy and the role of large data sets. 33rd AAAI Conference on Artificial Intelligence, AAAI 2019, 31st Innovative Applications of Artificial Intelligence Conference, IAAI 2019 and the 9th AAAI Symposium on Educational Advances in Artificial Intelligence, EAII 2019. AAAI Press; 2019:4039-4048. Accessed July 10, 2023. www.aaai.org
40. Taylor PN, Papasavvas CA, Owen TW, et al. Normative brain mapping of interictal intracranial EEG to localize epileptogenic tissue. *Brain.* 2022;145(3):939. Accessed February 4, 2023. <https://pubmed.ncbi.nlm.nih.gov/36373178/>
41. Thomas J, Kahane P, Abdallah C, et al. A subpopulation of spikes predicts successful epilepsy surgery outcome. *Ann Neurol.* 2022;93:522-535. Accessed February 1, 2023. <https://pubmed.ncbi.nlm.nih.gov/36373178/>
42. Bonilha L, Jensen JH, Baker N, et al. The brain connectome as a personalized biomarker of seizure outcomes after temporal lobectomy. *Neurology.* 2015;84(18):1846. Accessed February 4, 2023. <https://pubmed.ncbi.nlm.nih.gov/264433467/>
43. Taylor PN, Sinha N, Wang Y, et al. The impact of epilepsy surgery on the structural connectome and its relation to outcome. *Neuroimage Clin.* 2018;18:202-214. Accessed October 13, 2022. <https://pubmed.ncbi.nlm.nih.gov/35987798/>

44. Nissen IA, Millán AP, Stam CJ, et al. Optimization of epilepsy surgery through virtual resections on individual structural brain networks. *Sci Rep.* 2021;11(1):19025. Accessed December 13, 2021. <https://pubmed.ncbi.nlm.nih.gov/34561483/>
45. Lagarde S, Bénar C-G, Wendling F, Bartolomei F. Interictal functional connectivity in focal refractory epilepsies investigated by intracranial EEG. *Brain Connect.* 2022;12(10):850-869. Accessed February 4, 2023. <https://pubmed.ncbi.nlm.nih.gov/35972755/>
46. Gleichgerricht E, Keller SS, Drane DL, et al. Temporal lobe epilepsy surgical outcomes can be inferred based on structural connectome hubs: a machine learning study. *Ann Neurol.* 2020;88(5):970-983. doi:10.1002/ana.25888
47. Sinha N, Dauwels J, Kaiser M, et al. Predicting neurosurgical outcomes in focal epilepsy patients using computational modelling. *Brain.* 2017;140(2):319-332. Accessed December 13, 2021. <https://pubmed.ncbi.nlm.nih.gov/28011454/>
48. Wang HE, Woodman M, Triebkorn P, et al. Delineating epileptogenic networks using brain imaging data and personalized modeling in drug-resistant epilepsy. *Sci Transl Med.* 2023;15(680):eabp8982. Accessed February 4, 2023. <https://pubmed.ncbi.nlm.nih.gov/36696482/>
49. Ren L, Kucewicz MT, Cimbalknik J, et al. Gamma oscillations precede interictal epileptiform spikes in the seizure onset zone. *Neurology.* 2015;84(6):602-608. Accessed July 10, 2023. <https://pubmed.ncbi.nlm.nih.gov/25589669/>
50. Khan M, Chari A, Seunarine K, et al. Proportion of resected seizure onset zone contacts in pediatric stereo-EEG-guided resective surgery does not correlate with outcome. *Clin Neurophysiol.* 2022;138:18-24. Accessed February 5, 2023. <https://pubmed.ncbi.nlm.nih.gov/35364463/>
51. Weiss SA, Fried I, Wu C, et al. Graph theoretical measures of fast ripple networks improve the accuracy of post-operative seizure outcome prediction. *Sci Rep.* 2023;13(1):367. Accessed February 6, 2023. <https://www.nature.com/articles/s41598-022-27248-x>
52. Olmi S, Petkoski S, Guye M, et al. Controlling seizure propagation in large-scale brain networks. *PLoS Comput Biol.* 2019;15(2):e1006805. Accessed December 22, 2021. / [pmc/articles/PMC6405161/](https://pubmed.ncbi.nlm.nih.gov/34561483/).
53. An S, Bartolomei F, Guye M, Jirsa V. Optimization of surgical intervention outside the epileptogenic zone in the virtual epileptic patient (VEP). *PLoS Comput. Biol.* 2019;15(6):e1007051. Accessed December 22, 2021. / [pmc/articles/PMC6594587/](https://pubmed.ncbi.nlm.nih.gov/34561483/).
54. Conrad EC, Tomlinson SB, Wong JN, et al. Spatial distribution of interictal spikes fluctuates over time and localizes seizure onset. *Brain.* 2020;143(2):554-569. Accessed June 29, 2023. <https://pubmed.ncbi.nlm.nih.gov/31860064/>
55. Gliske SV, Irwin ZT, Chestek C, et al. Variability in the location of high frequency oscillations during prolonged intracranial EEG recordings. *Nat Commun.* 2018;9(1):2155. Accessed June 29, 2023. / [pmc/articles/PMC5984620/](https://pubmed.ncbi.nlm.nih.gov/31860064/).
56. Dellavale D, Bonini F, Pizzo F, et al. Spontaneous fast-ultradian dynamics of polymorphic interictal events in drug-resistant focal epilepsy. *Epilepsia.* 2023;64:2027-2043. Accessed June 29, 2023. <https://pubmed.ncbi.nlm.nih.gov/37199673/>